nature physics

ARTICLES

PUBLISHED ONLINE: 15 JANUARY 2012 | DOI: 10.1038/NPHYS2205

Fermionic transport and out-of-equilibrium dynamics in a homogeneous Hubbard model with ultracold atoms

Ulrich Schneider[1,2]*, Lucia Hackermüller[1,3], Jens Philipp Ronzheimer[1,2], Sebastian Will[1,2], Simon Braun[1,2], Thorsten Best[1], Immanuel Bloch[1,2,4], Eugene Demler[5], Stephan Mandt[6], David Rasch[6] and Achim Rosch[6]

Transport properties are among the defining characteristics of many important phases in condensed-matter physics. In the presence of strong correlations they are difficult to predict, even for model systems such as the Hubbard model. In real materials, additional complications arise owing to impurities, lattice defects or multi-band effects. Ultracold atoms in contrast offer the possibility to study transport and out-of-equilibrium phenomena in a clean and well-controlled environment and can therefore act as a quantum simulator for condensed-matter systems. Here we studied the expansion of an initially confined fermionic quantum gas in the lowest band of a homogeneous optical lattice. For non-interacting atoms, we observe ballistic transport, but even small interactions render the expansion almost bimodal, with a dramatically reduced expansion velocity. The dynamics is independent of the sign of the interaction, revealing a novel, dynamic symmetry of the Hubbard model.

In solid-state physics, transport properties are among the key observables, the most prominent example being the electrical conductivity, which, for example, allows one to distinguish normal conductors from insulators or superconductors. Furthermore, many of today's most intriguing solid-state phenomena manifest themselves in transport properties, examples including high-temperature superconductivity, giant magnetoresistance, quantum-Hall physics, topological insulators and disorder phenomena. Especially in strongly correlated systems, where the interactions between the conductance electrons are important, transport properties are difficult to calculate. In general, predicting out-of-equilibrium fermionic dynamics represents an even harder problem than the prediction of static properties such as the nature of the ground state. In real solids further complications arise owing to the effects, for example, of impurities, lattice defects and phonons. These complications render an experimental investigation in a clean and well-controlled ultracold-atom system highly desirable. Although recent years have seen dramatic progress in the control of quantum gases in optical lattices[1–3], a thorough understanding of the dynamics in these systems is still lacking. Genuine dynamical experiments can not only uncover new dynamic phenomena but are also essential to gain insight into the timescales needed to achieve equilibrium in the lattice[4,5] or to adiabatically load into the lattice[6,7].

Using both bosonic and fermionic[8–10] atoms, it has become possible to simulate models of strongly interacting quantum particles, for which the Hubbard model[11] is probably the most important example. A major advantage of these systems compared with real solids is the possibility to change all relevant parameters in realtime by, for example, varying laser intensities or magnetic fields. Although first studies of dynamical properties of both bosonic and fermionic[12–14] quantum gases have already been performed, a remaining key challenge, however, has been the presence of additional potentials on top of the periodic lattice potential: these will lead to confining forces or, in the absence of interactions, to Bloch oscillations[15–19] that dominate transport.

In this work, it was possible to study out-of-equilibrium dynamics and transport in a homogeneous Hubbard model by allowing an initially confined atomic cloud with variable interactions to expand freely within a homogeneous optical lattice (Fig. 1) without further potentials. Monitoring the *in situ* density distribution during the expansion led to several surprising observations: already small interactions cause a drastic reduction of mass transport within the expanding atomic cloud and change its shape; for strong interactions the core of the atomic cloud does not expand, but shrinks; and, surprisingly, we find that only the magnitude but not the sign of the interaction matters: the observed dynamics is identical for repulsive and attractive interactions despite a large difference in total energy.

The experiment starts with the preparation of a band-insulating state of fermionic potassium in a combination of a blue-detuned three-dimensional optical lattice and a red-detuned dipole trap (Methods). The applied lattice-loading procedure includes a hold time in a deep lattice with strongly reduced tunnelling, during which the interaction between the two used hyperfine states can be controlled using a Feshbach resonance. Combined with a strong harmonic confinement, this hold time causes a dephasing between different lattice sites and leads to a localization of the atoms to single lattice sites. This loading procedure results in a cloud of localized atoms with a constant density distribution, which is independent of

[1]Institut für Physik, Johannes Gutenberg-Universität, 55099 Mainz, Germany, [2]Fakultät für Physik, Ludwig-Maximilians-Universität, 80799 Munich, Germany, [3]School of Physics and Astronomy, University of Nottingham, NG7 2RD Nottingham, UK, [4]Max-Planck-Institut für Quantenoptik, 85748 Garching, Germany, [5]Department of Physics, Harvard University, Cambridge, Massachusetts 02138, USA, [6]Institut für Theoretische Physik, Universität zu Köln, 50937 Cologne, Germany. *e-mail: ulrich.schneider@lmu.de.

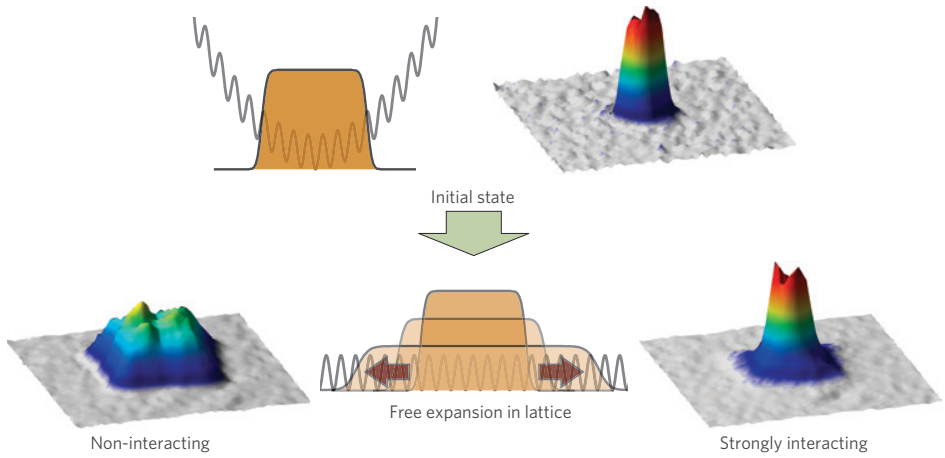

Figure 1 | Expansion of fermionic atoms after a quench of the trapping potential. First a dephased band-insulator is created in the combination of an optical lattice and a strong harmonic trap. Subsequently the harmonic confinement is switched off and the cloud expands in a homogeneous Hubbard model. The observed *in situ* density distributions demonstrate the strong effects of interactions on the evolution.

the chosen interaction (see Supplementary Information for details). Subsequently, the expansion is initiated by suddenly eliminating all confining potentials in the horizontal direction (Fig. 1). The resulting mass transport is not driven by an external potential but by density gradients. The applied preparation scheme guarantees that all interaction effects arise only during the expansion because the initial state is independent of the chosen interaction.

Non-interacting case

For non-interacting atoms, we observe that the symmetry of the cloud changes during the expansion from the rotational symmetry of the initial density distribution to a square symmetry that is governed by the symmetry of the lattice (Fig. 2).

In the absence of collisions and additional potentials the Hubbard Hamiltonian consists only of the hopping term $H_J = -J\sum_{\langle i,j\rangle}\hat{c}_i^\dagger\hat{c}_j$, which describes the tunnelling of a particle from one lattice site to a neighbouring site with a rate $J/\hbar$ ($\hat{c}_i^\dagger$ ($\hat{c}_i$) denotes the fermionic creation (destruction) operator). This Hamiltonian gives rise to a ballistic expansion where each initially localized particle expands independently with a constant quasi-momentum distribution. As a localized single-particle state (a Wannier function) is an equal superposition of all Bloch waves within the first Brillouin zone, the velocity distribution inherits the square symmetry of the Brillouin zone. This leads to the observed change in symmetry, as the density distribution after an evolution time t is given by the convolution of the initial density distribution (spherical) with the velocity distribution (square) of the individual atoms (classically: $\mathbf{r}(t) = \mathbf{r}(0) + \mathbf{v}t$; $\mathbf{v}$: possible velocity of an individual atom, $\mathbf{r}$: corresponding position). In the experiment, the width of a single-particle wavefunction (Fig. 2, dark blue dots), which is extracted from the images by deconvolving the observed cloud size with the initial cloud size, grows linearly with expansion time, thereby confirming the ballistic expansion. The extracted mean expansion velocity $v_{\mathrm{exp}} = \sqrt{\langle v^2\rangle}$ agrees very well with the quantum-mechanical prediction (solid line) $v_{\mathrm{exp}} = \sqrt{2d}\,(J/\hbar)a_{\mathrm{lat}}$ (d: dimension, a_{lat}: lattice constant), that is the averaged group velocity of the Bloch waves (see Supplementary Information). This expansion can be seen as a continuous quantum walk[20–24]. For comparison, classical (thermal) hopping of a particle (for example of a thermalized atom on the surface of a crystal) would result in a random walk, where the width of the resulting density distribution would scale as the square root of the expansion time (dashed lines). For very long expansion times, residual corrugations in the potential become relevant and can distort the square symmetry (see Supplementary Information).

Interacting case

The ballistic expansion observed for non-interacting atoms is in stark contrast to the interacting case, where a qualitatively different dynamics is observed: Fig. 3 shows *in situ* absorption images taken after 25 ms of expansion in an $8E_r$ deep lattice.

The observed dynamics gradually changes from a purely ballistic expansion in the non-interacting case into an almost bimodal expansion for interacting atoms: on increasing $|U|$, larger and larger parts of the cloud remain spherical (clearly seen in Fig. 1) and only a small fraction of atoms in the tails of the cloud exhibits a square distribution. Here U denotes the strength of the on-site interaction between different spin components ($H_{\mathrm{I}} = U\sum_i \hat{n}_{i,\downarrow}\hat{n}_{i,\uparrow}$). The spherical shape is a consequence of frequent collisions between the atoms in the centre of the cloud, which, for the range of interactions considered here, drive the system to be close to local thermal equilibrium[25,26]: within the rather large clouds used in the experiment, gradients are small and the dynamics in the centre can be described by coupled nonlinear diffusion equations[27] for density $n(\mathbf{r},t)$ and local energy $e(\mathbf{r},t)$

$$\partial_t \mathbf{n} = \nabla D(\mathbf{n})\nabla\mathbf{n} \qquad (1)$$

where $\mathbf{n} = (n, e)$ and $D(\mathbf{n})$ is a 2×2 matrix of diffusion constants. Note that in the optical lattice frequent Umklapp scattering prohibits convective terms in the hydrodynamic equation (equation (1)). Because the diffusion equation is rotationally invariant, a diffusive dynamics can directly account for the observed spherical shape of the high-density core.

For a theoretical description it is essential to realize that the diffusion equation (equation (1)) is highly singular. As the diffusion constant is proportional to the scattering time, it diverges as $1/n$ for small densities, $D(\mathbf{n}) \sim 1/n$, as the probability to scatter from other atoms is linear in n for small densities. Such highly singular 'superfast' diffusion equations have been extensively studied in the mathematical literature[28]. Remarkably, they predict a completely unphysical behaviour in large dimensions ($d \geq 2$): the particle number is not conserved, as particles vanish at infinity with a constant rate (for $d = 2$). Owing to this breakdown of the hydrodynamic approach, the expansion is not governed by the diffusion equation but instead by the physics in the tails of the cloud where no local equilibrium can be reached. In this regime, the densities are low and atoms scatter so rarely that their motion again becomes ballistic. Therefore the tails of the cloud show the square symmetry characteristic for freely expanding particles (Fig. 3). This initial fraction of ballistically expanding atoms decreases for

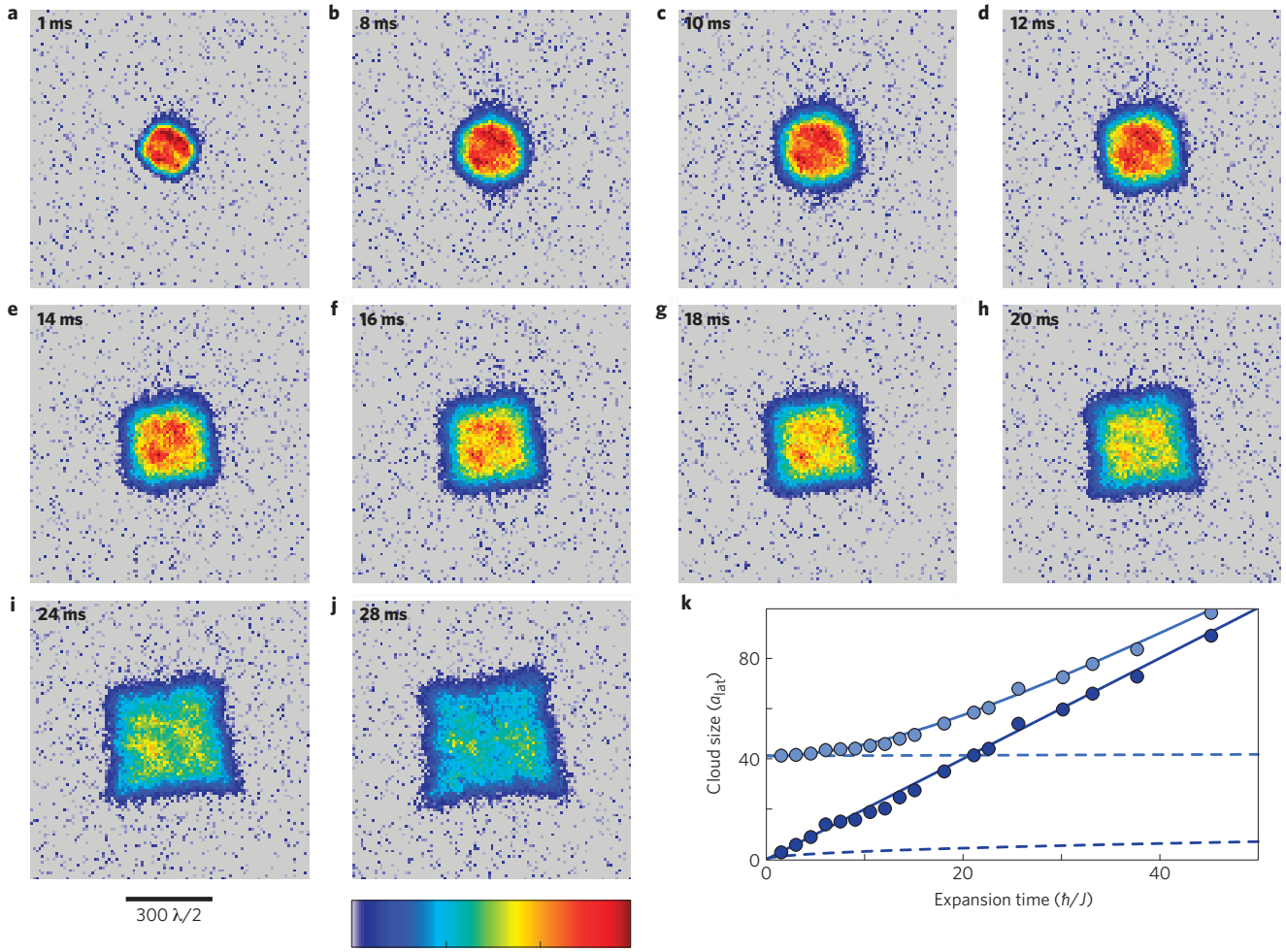

Figure 2 | Expansion of non-interacting fermions. a–j, *In situ* absorption images (column density in a.u.) of an expanding non-interacting cloud in a horizontally homogeneous square lattice with lattice depth $8E_r$ ($1\,\mathrm{ms} \approx 1.8\hbar/J$). The expansion changes the symmetry of the cloud from the rotational symmetry of the harmonic trap to the square symmetry of the lattice Brillouin zone. **k**, Fitted cloud size $R(t)$ (light) and deconvolved single particle width $R_s(t) = \sqrt{R(t)^2 - R(0)^2}$ (dark) extracted from phase-contrast images. Solid lines denote the quantum mechanical prediction and the dashed lines a corresponding classical random walk.

increasing interaction strengths. During the expansion the density gets reduced and, in the limit of infinite expansion times, all atoms are expected to become ballistic. This crossover into ballistic behaviour for small densities leads to a breakdown of the diffusive behaviour and regularizes the otherwise singular diffusion equation.

To describe both the diffusive and the ballistic regime, we use numerical simulations based on the semi-classical Boltzmann equation in the relaxation-time approximation:

$$\partial_t f_{\mathbf{q}} + \mathbf{v}_{\mathbf{q}} \nabla_{\mathbf{r}} f_{\mathbf{q}} + \mathbf{F}(\mathbf{r}) \nabla_{\mathbf{q}} f_{\mathbf{q}} = -\frac{1}{\tau(\mathbf{n})} \left(f_{\mathbf{q}} - f^0_{\mathbf{q}}(\mathbf{n}) \right) \qquad (2)$$

This equation describes the evolution of a semi-classical momentum distribution $f_{\mathbf{q}}(\mathbf{r}, t)$ as a function of position and time in the presence of a force $\mathbf{F}$. Here, the transport scattering time $1/\tau(\mathbf{n})$, which describes the relaxation towards an equilibrium Fermi distribution $f^0_{\mathbf{q}}$ for given energy and particle densities, is determined from a microscopic calculation of the diffusion constant for small interactions (see Supplementary Information for details). The Boltzmann equation describes qualitatively and semi-quantitatively the observed cloud shapes, see Fig. 3b.

The core width $R_c(t)$, which measures the size of only the high-density core, is extracted from phase-contrast images by determining the half-width at half-maximum (HWHM) of the density distribution (see Supplementary Information). By fitting the evolving core width to $R_c(t) = \sqrt{R_{c,0}^2 + v_c^2 t^2}$, we extract the core expansion velocities v_c, which are shown in Fig. 4. Surprisingly, they decrease dramatically already for interactions much smaller than the bandwidth 8 J, which highlights the strong impact of moderate interactions on mass transport in these systems. We observe the same behaviour irrespective of the sign of the interactions.

For interactions larger than $|U/J| \gtrsim 3$, the dynamics of the high-density core changes qualitatively: the core starts shrinking instead of expanding and the core expansion velocities v_c become negative. In this regime, the expansion of the diffusive core is strongly suppressed and the essentially frozen core dissolves by emitting ballistic particles and therefore shrinks in size, similarly to a melting ball of ice. This feature is also recovered by our simulations based on the Boltzmann equation (red line in Fig. 4). The slight asymmetry at large interactions can be attributed to interaction-dependent losses caused by light-assisted collisions during the preparation sequence. Note that the suppressed expansion is not related to any self-trapping arising from the interaction potential[29], as we have checked by switching off the corresponding forces in our numerical simulations.

This pronounced dependence of the dynamics on small interactions enabled us to measure the zero crossing of the scattering length ($B(a = 0) = 209.1 \pm 0.2\,\mathrm{G}$), which corresponds to a width of the Feshbach resonance of $w = 7.0 \pm 0.2\,\mathrm{G}$, see

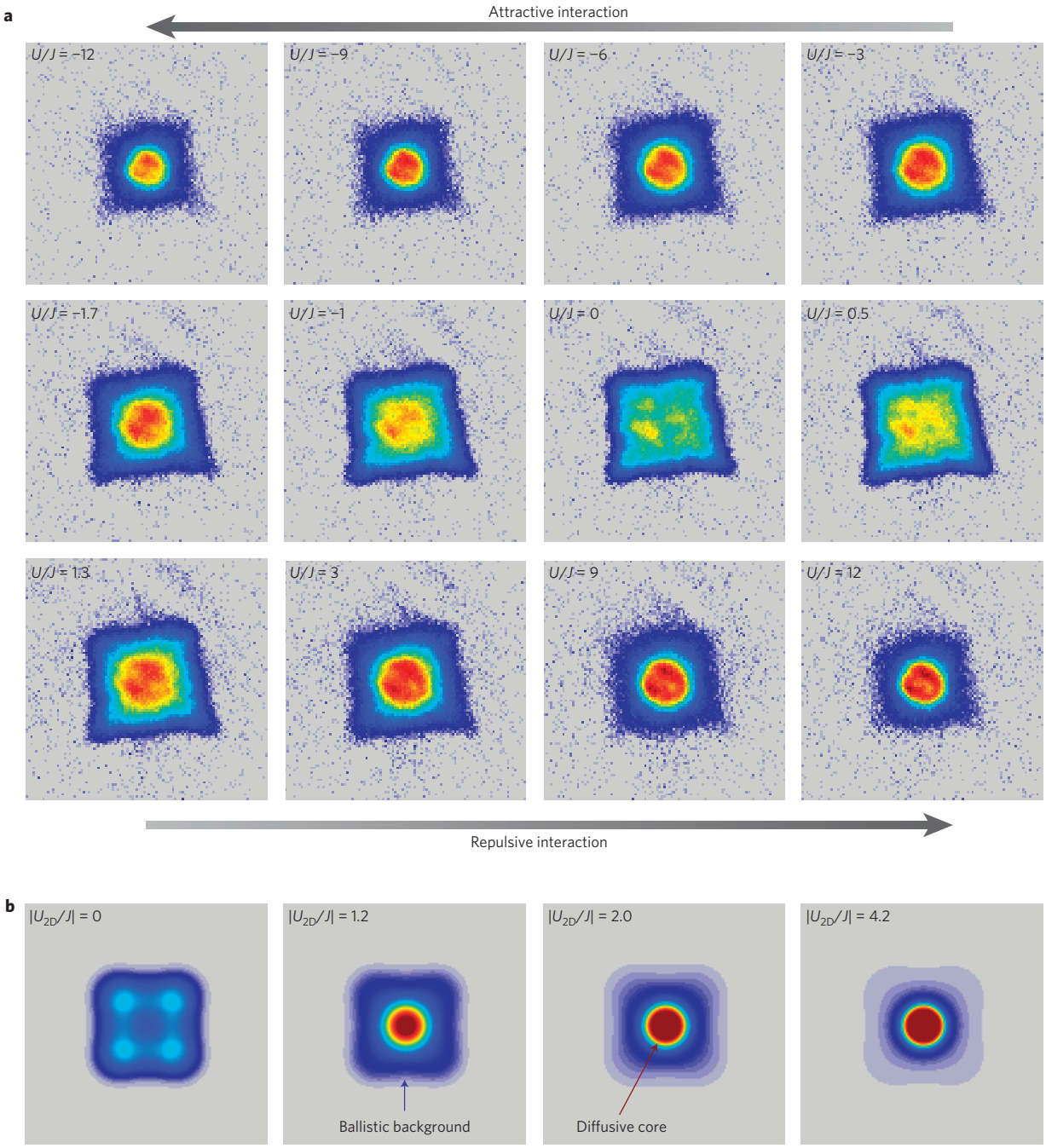

Figure 3 | Expansion of interacting fermions. a, Experimental *in situ* absorption images for different interactions after 25 ms expansion in a horizontally homogeneous lattice. The images show a symmetric crossover from a ballistic expansion for non-interacting clouds to an interaction-dominated expansion for both attractive and repulsive interactions. Images are averaged over at least five shots and all scales are identical to those in Fig. 2. **b**, Simulated density distributions using a 2D Boltzmann equation.

Supplementary Information. In contrast to the high interaction limit, where the exponentially long lifetime[5] of excess doublons leads to two independent dynamics of doublons and single atoms, we observe thermal equilibrium between doublons and unpaired atoms, as shown in detail in the Supplementary Information.

We have shown that the observed transport properties can be qualitatively predicted by the semi-classical Boltzmann equation (equation (2)). However, the full quantum dynamics is certainly more complex and includes, for example, the formation of entanglement between distant atoms[30] as well as the existence of bound or repulsively bound states. Although the expansion can be modelled in 1D (ref. 31) using DMRG methods[32], so far no methods are available to calculate the dynamics quantum-mechanically in higher dimensions. The separation between ballistically expanding atoms carrying high entropy and the high-density core in the centre could be used to locally cool the atoms via quantum-distillation processes[33].

Surprisingly, we observe identical density profiles and expansion rates for repulsive and attractive interactions of the same strength (Figs 3, 4). Whereas scattering cross sections are proportional to U^2 for small U, the interaction energy and density gradients give rise to forces linear in U: repulsive interactions create a positive pressure, which in free space would lead to an increased expansion rate, whereas an attractive interaction is

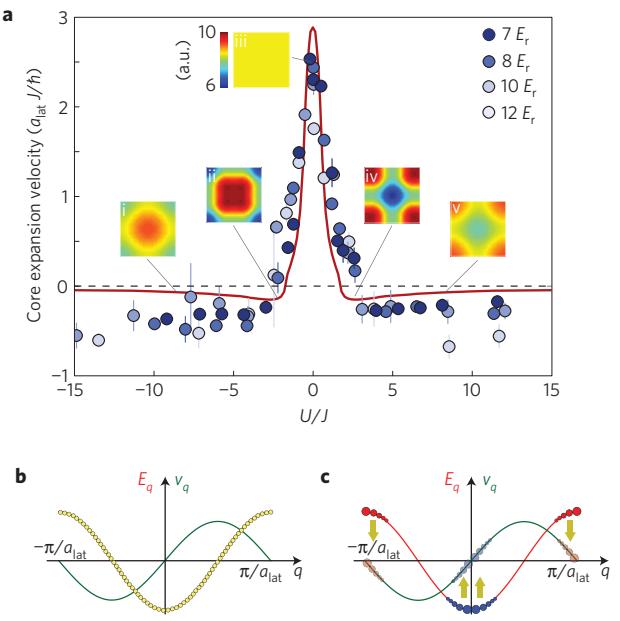

Figure 4 | Core-expansion velocities. a, Measured core-expansion velocities versus interaction for various lattice depths in a 2D situation (vertical lattice depth $20E_r$). The red line denotes the result of a numerical calculation (see text) and the error bars indicate the 1σ statistical fit uncertainty. The insets i–v show the numerically calculated quasi-momentum distribution after 40 ms of expansion for $U/J = -8, -2, 0, 2, 8$, respectively. **b**,**c**, 1D energy dispersion (red line) and group velocity (green line) together with schematic sketches of the relative occupations (yellow: initial state (**b**) and $U = 0$, red: $U > 0$ (**c**), blue: $U < 0$ (**c**)): although the quasi-momentum distribution is different for U and $-U$, the resulting group-velocity distribution (shaded) is identical.

expected to slow down the expansion, in contrast to the observed behaviour in the lattice.

The identical evolution of the density for positive and negative U is the consequence of an exact dynamical symmetry of the Hubbard model, which relies on two facts: first, if both the initial state and the observable are invariant under time reversal symmetry, the dynamics of the observable is necessarily unchanged by the transformation $H \rightarrow -H$. Second, as $\epsilon_{\mathbf{q}} = -2J\sum_i \cos(q_i d)$ is the kinetic energy of the Hubbard model, the sign of the hopping J can be changed, $J \rightarrow -J$, by shifting all momenta $\mathbf{q} \rightarrow \mathbf{q} + (\pi, \pi, \pi)/d$. When now both the initial state and the observable are invariant under both time reversal and the above shift of momenta, one necessarily obtains the same evolution for U and $-U$. This is the case in our experiment, initially all particles are localized and all momenta are therefore equally occupied while the density operator is time-reversal symmetric and momentum independent. A formal proof of this argument is given in the Supplementary Information.

During the expansion, when the density of atoms is reduced, interaction energy is converted into kinetic energy. Initially the kinetic energy of the localized particles is zero. For $U < 0$, the total energy is therefore negative and low momentum states become more populated during the expansion. For $U > 0$, in contrast, the total energy is positive, implying an enhanced occupation of higher momentum states. More precisely, the two momentum distributions for U and $-U$ are shifted by $(\pi, \pi, \pi)/d$, as can be seen in the insets i–v in Fig. 4. In free space, where $\epsilon_{\mathbf{q}} \sim q^2$, larger momenta imply larger group velocities $\mathbf{v_q} = (1/\hbar)\, d\epsilon_{\mathbf{q}}/d\mathbf{q} \sim q$ and the cloud expands faster for repulsive interactions. For the Hubbard model, in contrast, the group velocities for $\mathbf{q}$ and $(\pi, \pi, \pi)/d - \mathbf{q}$ are the same, $v^i_{q_i} \sim \sin q_i d$, leading to the same expansion of the cloud for U and $-U$, see Fig. 4b,c.

As large parts of the cloud are expected to be in local equilibrium in the interacting case, one can define local temperatures: for $U < 0$ the system cools down while expanding and positive local temperatures $0 < T(r) < \infty$ are obtained. For $U > 0$, in contrast, the exact dynamical symmetry implies that the local temperatures have to be negative, as $\exp[-H/k_B T] = \exp[-(-H)/(-k_B T)]$. This has also been confirmed by our numerical calculations (Supplementary Fig. S3). Negative temperatures describe equilibrated systems with population inversion and are well defined for systems such as the Hubbard model where the energy has an upper bound[34]. They have been observed in spin systems[35] and localized ultracold atoms[36]. Assuming local thermalization, the observed $U \leftrightarrow -U$ symmetry directly implies negative temperatures for repulsive interactions at long expansion times.

Conclusion

Ultracold fermions in optical lattices offer many unique possibilities to study non-equilibrium dynamics, as they allow for a full real-time control of almost all relevant parameters, including quantum quenches, where the Hamiltonian of the system is changed instantaneously. We studied the expansion of a cloud of initially localized atoms in a homogeneous Hubbard model following a quench of the trapping potential and observed the crossover from a ballistic expansion at small densities or vanishing interactions to a bimodal expansion in the interacting case. We observed identical behaviour for both attractive and repulsive interactions, highlighting the high symmetry of the kinetic energy in the Hubbard model. The surprisingly large observed timescales of mass transport set lower limits on the timescales needed both to adiabatically load the atoms into the lattice and to cool the system in the lattice[37] and are therefore of paramount importance for all attempts to create complex, strongly correlated many-body states such as Néel-ordered states in these systems.

The method of directly measuring the expansion dynamics can be used to detect complex quantum states, including Mott-insulating states[10], or to possibly distinguish pseudogap[8] from superfluid states in the attractive Hubbard model. In addition, the effects of various disorder potentials on the two-dimensional dynamics can be studied. The extension to a Bose–Fermi mixture could enable studies on ohmic transport, where the bosons assume the role of the phonons.

Methods

Experimental sequence. We use a balanced spin mixture of the two lowest hyperfine states $|F, m_F\rangle = |9/2, -9/2\rangle$ and $|9/2, -7/2\rangle$ of fermionic potassium ^{40}K with $N = 2\text{–}3 \times 10^5$ atoms at an initial temperature of $T/T_F = 0.13(2)$. Starting in an harmonic trap, the atoms are loaded into a combination of a blue-detuned three-dimensional optical lattice with lattice constant $a_{lat} = \lambda/2 = 369$ nm and a red-detuned dipole trap, using a sequence similar to the one applied in ref. 10. Once in the lattice, tunnelling is strongly reduced by increasing the lattice depth to $20E_r$ (recoil energy $E_r = h^2/(2m\lambda^2)$) and the interactions can be controlled via a Feshbach resonance without affecting the density distribution (see Supplementary Information). To initiate the expansion, the lattice depth is lowered again and the harmonic confinement (see Fig. 1a) along the horizontal directions is eliminated by reducing the strength of the dipole trap by more than 90%, such that along the horizontal directions the remaining dipole potential precisely compensates the anti-confinement produced by the lattice beams (see Supplementary Information).

Whereas any vertical motion is expected to be strongly suppressed by gravity-induced Bloch oscillations (oscillation amplitude $2\,\mathrm{J\,(mg)^{-1}} < 2\,d$), the atoms are exposed to a homogeneous Hubbard model without additional potentials in the horizontal directions. The evolution of the density distribution during the following expansion was monitored by *in situ* imaging along the vertical axis of the cloud, thereby integrating over any vertical dynamics. Absorption images of the resulting dynamics are shown in Fig. 2 for the case of non-interacting particles and in Fig. 3 for various interactions.

For a quantitative analysis (Figs 2k and 4; Supplementary Information), vertical tunnelling of the atoms during the expansion was further suppressed by increasing the depth of the vertical lattice to $20E_r$, thereby realizing several layers of independent two-dimensional Hubbard models. All quantitative analyses were performed using phase-contrast images.

Received 23 August 2011; accepted 9 December 2011; published online 15 January 2012

References

1. Jaksch, D. & Zoller, P. The cold atom Hubbard toolbox. *Ann. Phys.* **315,** 52–79 (2005).
2. Lewenstein, M. *et al.* Ultracold atomic gases in optical lattices: Mimicking condensed matter physics and beyond. *Adv. Phys.* **56,** 243–379 (2007).
3. Bloch, I., Dalibard, J. & Zwerger, W. Many-body physics with ultracold gases. *Rev. Mod. Phys.* **80,** 885–964 (2008).
4. Hung, C., Zhang, X., Gemelke, N. & Chin, C. Slow mass transport and statistical evolution of an atomic gas across the superfluid-Mott-insulator transition. *Phys. Rev. Lett.* **104,** 160403 (2010).
5. Strohmaier, N. *et al.* Observation of elastic doublon decay in the Fermi–Hubbard model. *Phys. Rev. Lett.* **104,** 080401 (2010).
6. Wernsdorfer, J., Snoek, M. & Hofstetter, W. Lattice-ramp-induced dynamics in an interacting Bose–Bose mixture. *Phys. Rev. A* **81,** 043620 (2010).
7. Gericke, T. *et al.* Adiabatic loading of a Bose–Einstein condensate in a 3D optical lattice. *J. Mod. Opt.* **54,** 735–743 (2007).
8. Hackermüller, L. *et al.* Anomalous expansion of attractively interacting fermionic atoms in an optical lattice. *Science* **327,** 1621–1624 (2010).
9. Jördens, R., Strohmaier, N., Günter, K., Moritz, H. & Esslinger, T. A Mott insulator of fermionic atoms in an optical lattice. *Nature* **455,** 204–207 (2008).
10. Schneider, U. *et al.* Metallic and insulating phases of repulsively interacting fermions in a 3D optical lattice. *Science* **322,** 1520–1525 (2008).
11. Hubbard, J. Electron correlations in narrow energy bands. *Proc. R. Soc. A* **276,** 238–257 (1963).
12. Pezzè, L. *et al.* Insulating behavior of a trapped ideal Fermi gas. *Phys. Rev. Lett.* **93,** 120401 (2004).
13. Ott, H. *et al.* Collisionally induced transport in periodic potentials. *Phys. Rev. Lett.* **92,** 160601 (2004).
14. Strohmaier, N. *et al.* Interaction-controlled transport of an ultracold Fermi gas. *Phys. Rev. Lett.* **99,** 220601 (2007).
15. Lignier, H. *et al.* Dynamical control of matter-wave tunneling in periodic potentials. *Phys. Rev. Lett.* **99,** 220403 (2007).
16. Ben Dahan, M., Peik, E., Reichel, J., Castin, Y. & Salomon, C. Bloch oscillations of atoms in an optical potential. *Phys. Rev. Lett.* **76,** 4508–4511 (1996).
17. Fertig, C. D. *et al.* Strongly inhibited transport of a degenerate 1D Bose gas in a lattice. *Phys. Rev. Lett.* **94,** 120403 (2005).
18. Gustavsson, M. *et al.* Control of interaction-induced dephasing of Bloch oscillations. *Phys. Rev. Lett.* **100,** 080404 (2008).
19. Fattori, M. *et al.* Atom interferometry with a weakly interacting Bose–Einstein condensate. *Phys. Rev. Lett.* **100,** 080405 (2008).
20. Aharonov, Y., Davidovich, L. & Zagury, N. Quantum random walks. *Phys. Rev. A* **48,** 1687–1690 (1993).
21. Farhi, E. & Gutmann, S. Quantum computation and decision trees. *Phys. Rev. A* **58,** 915–928 (1998).
22. Karski, M. *et al.* Quantum walk in position space with single optically trapped atoms. *Science* **325,** 174–177 (2009).
23. Weitenberg, C. *et al.* Single-spin addressing in an atomic Mott insulator. *Nature* **471,** 319–324 (2011).
24. Childs, A. M. *et al.* in *STOC '03: Proceedings of the Thirty-Fifth Annual ACM Symposium on Theory of Computing* 59–68 (2003).
25. Rigol, M., Dunjko, V. & Olshanii, M. Thermalization and its mechanism for generic isolated quantum systems. *Nature* **452,** 854–858 (2008).
26. Eckstein, M., Kollar, M. & Werner, P. Thermalization after an interaction quench in the Hubbard model. *Phys. Rev. Lett.* **103,** 056403 (2009).
27. Mandt, S., Rapp, A. & Rosch, A. Interacting fermionic atoms in optical lattices diffuse symmetrically upwards and downwards in a gravitational potential. *Phys. Rev. Lett.* **106,** 250602 (2011).
28. Vázquez, J. L. *Smoothing and Decay Estimates for Nonlinear Diffusion Equations* (Oxford Univ. Press, 2006).
29. Anker, Th. *et al.* Nonlinear self-trapping of matter waves in periodic potentials. *Phys. Rev. Lett.* **94,** 020403 (2005).
30. Romero-Isart, O., Eckert, K., Rodo, C. & Sanpera, A. Transport and entanglement generation in the Bose–Hubbard model. *J. Phys. A* **40,** 8019–8031 (2007).
31. Kajala, J., Massel, J. & Törmä, P. Expansion dynamics in the one-dimensional Fermi–Hubbard model. *Phys. Rev. Lett.* **106,** 206401 (2011).
32. Schollwöck, U. The density matrix renormalization group. *Rev. Mod. Phys.* **77,** 259–315 (2005).
33. Heidrich-Meisner, F. *et al.* Quantum distillation: Dynamical generation of low-entropy states of strongly correlated fermions in an optical lattice. *Phys. Rev. A* **80,** 041603 (2009).
34. Rapp, A., Mandt, S. & Rosch, A. Equilibration rates and negative absolute temperatures for ultracold atoms in optical lattices. *Phys. Rev. Lett.* **105,** 220405 (2010).
35. Purcell, E. M. & Pound, R. V. A nuclear spin system at negative temperature. *Phys. Rev.* **81,** 279–280 (1951).
36. Medley, P., Weld, D. M., Miyake, H., Pritchard, D. E. & Ketterle, W. Spin gradient demagnetization cooling of ultracold atoms. *Phys. Rev. Lett.* **106,** 195301 (2011).
37. McKay, D. C. & DeMarco, B. Cooling in strongly correlated optical lattices: Prospects and challenges. *Rep. Prog. Phys.* **74,** 054401 (2011).

Acknowledgements

We thank M. Moreno-Cardoner, F. Heidrich-Meisner, D. Pekker and R. Sensarma, B. Kawohl, C. Kiefer, J. Krug and M. Zirnbauer for stimulating and insightful discussions. This work was supported by the Deutsche Forschungsgemeinschaft (FOR801, SFB TR 12, SFB 608, Gottfried Wilhelm Leibniz Prize), the European Union (Integrated Project SCALA), EuroQUAM (L.H.), the US Defense Advanced Research Projects Agency (Optical Lattice Emulator program), the US Air Force Office of Scientific Research (Quantum Simulation MURI (E.D.)), the National Science Foundation (DMR-07-05472) (E.D.), the Harvard-MIT CUA (E.D.), MATCOR (S.W.), the Gutenberg Akademie (S.W.) and the German National Academic Foundation (S.M.).

Author contributions

U.S., L.H. and J.P.R. carried out the measurements, U.S. performed the data analysis with contributions from L.H. and J.P.R.. I.B. supervised the measurements. S.M. and D.R. performed the numerical calculations supervised by A.R.. E.D., U.S. and A.R. constructed the analytical proof of the dynamical symmetry. U.S. and A.R. wrote the manuscript with substantial contributions by I.B. and all authors.

Additional information

The authors declare no competing financial interests. Supplementary information accompanies this paper on www.nature.com/naturephysics. Reprints and permissions information is available online at www.nature.com/reprints. Correspondence and requests for materials should be addressed to U.S.